

RETRIEVAL OF BOUNDARY LAYER AND CLOUD BASE HEIGHTS IN MANILA FROM A TWO-WAVELENGTH LIDAR MEASUREMENT

Maria Cecilia D. Galvez¹, Ernest P. Macalalad² and Edgar A. Vallar¹

¹Physics Department, De La Salle University, 2401 Taft Ave., Malate, Manila, Philippines 1004 ; Tel :+632-5360229
Email : maria.cecilia.galvez@dlsu.edu.ph

²Graduate Student, Institute of Space Science, National Central University, No. 300 Jhongda Rd., Jhongli City, Taoyuan County, 32001, Taiwan
Email: 986403601@cc.ncu.edu.

KEY WORDS: aerosol, boundary layer, cloud height, lidar

ABSTRACT: The boundary layer and cloud heights were determined from two wavelength lidar measurement in Manila. Normalized concentration gradient (NCG) method was implemented in the boundary layer height retrieval and from the slope of the range squared corrected signal (RSCS), the cloud base heights were retrieved. During the time of the measurement from 1500 to 2200 HR local time, the boundary layer height was found to be stable at around 370 m, which is considered as period of stable stratification. The cloud heights from the slope method during the measurement period was 800 m up to 1.2 km and the other layer starting from 1.6 km to 1.8 km. The calculated cloud heights matched the clouds that can be determined visually from the range-squared corrected signal THI plot.

1. INTRODUCTION

The mixed layer is usually defined as the turbulence region extending above the surface in which the mixing of air properties takes place (Stull,1988). It is generally regarded as an important link between the Earth's surface and the free atmosphere. Knowledge of the vertical profiles of momentum, heat and moisture is needed to fully understand this link. The mixed layer is also of particular importance to air pollution. Accurate incorporation of the mixed layer height (MLH) is crucial for photochemical and dispersion models to accurately predict pollutant concentrations. Conventionally, observation of the mixed layer structure is made by means of balloons, sondes, and acoustic sounders. In the mixed layer, air is typically moister and has greater aerosol content than in the free atmosphere, which results in more scattering of laser light, and a LIDAR can easily detect the boundary between the two layers (Kunkel et.al., 1977)(Boers et. al., 1984)(Melfi et. al., 1985). A number of studies have focused on the comparison between LIDAR measurements and other conventional measurements, and in general, the LIDAR technique is considered to be suitable for estimating the mixed layer height (Coulter, 1979)(Marsik et. al., 1995). Since the mixed layer is directly influenced by the Earth's surface, its thickness is widely variable according to the time of day and the season. In order to understand the characteristics of the mixed layer, it is necessary to observe it on a long-term basis. In this paper, we determine the boundary layer height from two-wavelength LIDAR measurement using the Normalized Concentration Gradient (NCG) Method and the cloud base heights from the slope of the range-squared corrected signal (RSCS).

2. METHOD

2.1 The Normalized Concentration Gradient Method

The method used in determining the boundary layer height (BLH) from our LIDAR data is briefly described here. The starting point in studying the evolution of the atmospheric boundary layer is getting the range-squared-corrected signal (RSCS) which is defined as

$$RSCS = (RS - RS_o) r^2 \quad (1)$$

where and RS_o is the background signal.

The boundary layer is characterized by the abundant presence of aerosols. Thus, the boundary layer height (BLH) can be observed in the altitude where there is a sudden drop in aerosol concentration. In this way, the BLH can also be determined from the normalized concentration gradient (NCG) in which is defined as the height near the surface where the NCG is a maximum and positive and above which it continues to be negative (Sasano et. al., 1982)(Sasano, 1985). In the NCG method, the amount of concentration of the two nearest neighbors are compared for a particular

altitude in the atmosphere, if it satisfies a certain criterion (which is a change of 0.8% - 1.1% concentration per meter), the point in that altitude will be considered as part of the boundary layer. The NCG is given as

$$NCG(R_i) = - \frac{C(R_{i+1}) - C(R_{i-1})}{C(R_i)(R_{i+1} - R_{i-1})} \times 100 \text{ (\%/m)} \quad (2)$$

where $C(R_i)$ is the particle concentration at altitude R_i , R_{i+1} is the altitude higher than R_i by one range resolution and R_{i-1} is the altitude lower than R_i by one range resolution. In this study, the NCG value will be varied from 0.8% to 1.1% depending on the response of the data to the variation. Since an increase in particle concentration would also mean an increase in the backscattered intensity signal, the RSCS will be used in Eq. (2) in place of the concentration.

2.2 Cloud Based Height Determination

Clouds and aerosols detected by the LIDAR system are denoted by peaks after the overlap peak in the LIDAR or the range-squared corrected signal (RSCS). The overlap peak is the peak at which the LIDAR signal starts to be detected by the telescope. It is not easy for an observer to readily determine whether the peak in the signal is caused by a cloud or an aerosol. But, usually, a cloud is a peak in the signal located at a height greater than 1 km, while aerosols are typically located at heights less than 1 km. The RSCS was used instead of the LIDAR signal because the peaks in the RSCS are much higher than in the LIDAR signal. Also, the overlap is not present in the RSCS.

After determining whether a peak is a cloud or not, the next procedure to perform is to smoothen the RSCS. Moving average was applied twice in order to smoothen the signal. Then, the slope of the RSCS was taken. The slope will be used in order to determine the cloud base height, the cloud peak height, and the cloud top height. Cloud base height is defined to be the point at which the RSCS starts to rise. This is an equivalent of a rise in the slope. The zero before the slope begins to rise is a candidate for the cloud base height. But before it can be marked as a cloud base height, a criterion should first be satisfied. The criterion is that after the candidate point, the next set of points before the next zero value should all be positive values. This means that the slope should be a positive peak. The number of points per set will depend on how noisy the signal is. If the conditions are satisfied, the equivalent height at that zero slope will be marked as a cloud base height.

2.3 The DLSU Two-Wavelength LIDAR System

The DLSU two-wavelength slant path LIDAR system measures backscatter signal at two wavelengths 355 and 532 nm with depolarization measurement at 532 nm. The laser transmitter is a frequency tripled ND:YAG laser with a pulse repetition frequency of 20 Hz. A Newtonian telescope, with a diameter of 200 mm and a focal length of 800 mm, collects the backscattered beam and directs it to a fully optically enclosed receiver assembly containing the receiving optics. Currently, the LIDAR system is situated at the 3rd floor of the DLSU Science and Technology Research Center (STRC) in Manila. It is aimed along the direction of 12° East of South of the LIDAR site towards the Pasay City area, passing over busy roads such as Vito Cruz, Gil Puyat Avenue and Libertad. The LIDAR site is just only 900 meters from Manila bay. Table 1 summarizes the specifications of the components of the system that was used in the study.

Table 1. Specification of the DLSU Lidar System.

Laser			Detectors		
Wavelength	532 nm	355 nm	Type	PMT	PMT
Model	Continuum I-20 Nd:YAG		Model	Hamamatsu R928	Hamamatsu R943-02
Output Energy (mJ)	175	125	Spectral Range	185 to 900 nm	160 to 930 nm
Pulse Repetition Frequency	20 Hz		Quantum efficiency	18%	22%
Pulse duration (ns)	5 - 7		Data Acquisition		
Beam divergence (mrad)	0.5		Oscilloscope	Agilent 54621D MSO	
Telescope			Osc. Sampling rate	100, 200 MSa/s	
Type	Newtonian		Resolution	8,16 bit (byte/word)	
Diameter	200 mm		Personal computer	Intel Celeron 333 MHz processor	
Focal Length	800 mm		Communication	Serial (COM1 and COM2)	
Iris diameter	approx. 2 mm		Averaging	variable: 128 to 2048, max is 16384	
Optical Filters					
Type	Narrow bandpass filter				
Peak wavelength	532.5 nm	356.4 nm			
Bandwidth	3 nm	10 nm			
Transmission	60%	25%			

3. RESULTS

3.1 Boundary Layer Height

The NCG method in determining the BLH is applied to Lidar experiments conducted in the afternoon of March 23, 2004 (1500HR to 2200HR LST) and in the morning of March 24, 2004 (0429HR to 1003HR LST). Shown in figures 1a and 1b are the time series of the RSCS from 355 nm backscatter signal on March 23 and March 24, respectively. March 23 observation period started at 1500HR, which was after the period of unstable thermal stratification. A residual of the mixed layer is observed from figure 1. The mixed layer had a height of 600 m until it gradually decreases to 400 m at around 1830HR and 200 m at the end of the observation period. In the morning of the following day March 24, the same layer from the previous night can be observed and at around 0600HR starts to increase to about 400m as traffic starts to build up around this time. Using the backscatter signal from 355 nm the calculated boundary layer heights from the two sets of Lidar measurements are also presented in time series on figures 3a and 3b. It can be seen from figures 3a and 3b that the boundary layer height determined from NCG method for the two different dates are rather stable all throughout the observation period. An almost constant BLH of about 400 m were measured from the two LIDAR observation periods. The BLH seems to vary a little on March 24 from 400m to 300m. These time periods are described as a period of stable stratification (Menuet et. al., 1999).

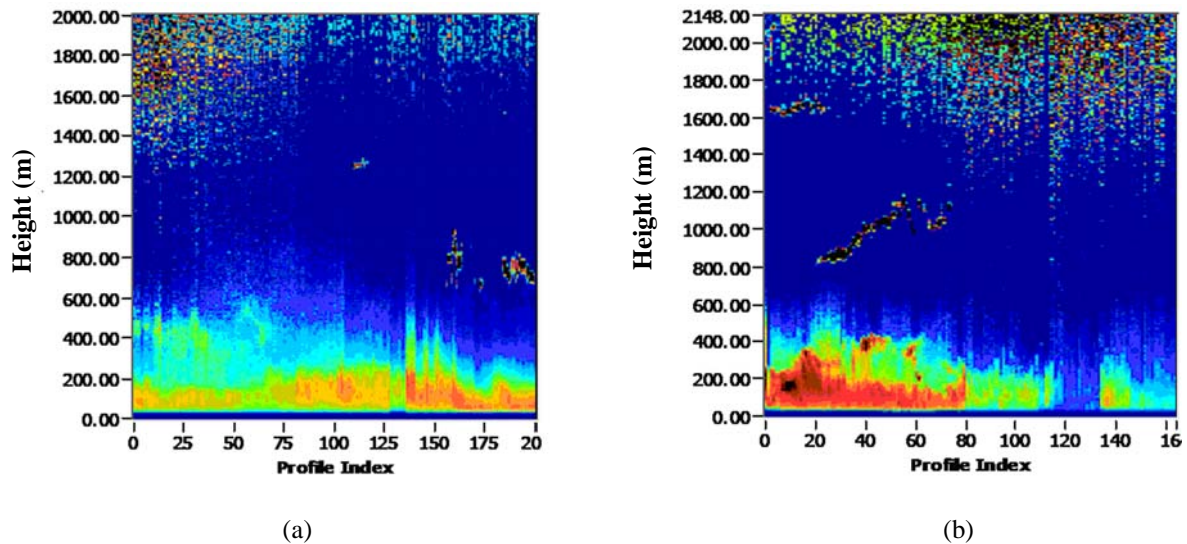


Figure 1. (a) Time series of the RSCS from 355 nm backscatter signal on March 23, 2004 from 1500HR to 2200HR local standard time (LST). (b) Time series of the RSCS from 355 nm backscatter signal on March 24, 2004 from 0429HR to 1003HR local standard time (LST).

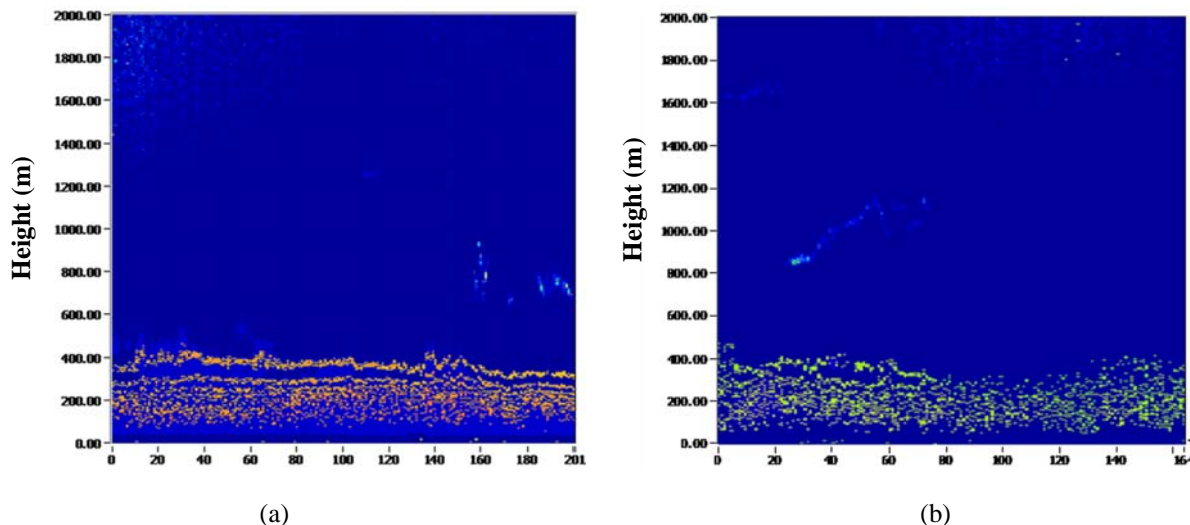


Figure 2. (a) Time series of the calculated boundary layer height from 355 nm backscatter signal on March 23, 2004 from 1500HR to 2200HR local standard time (LST). (b) Time series of the calculated boundary layer height from 355 nm backscatter signal on March 24, 2004 from 0429HR to 1003HR local standard time (LST).

3.2 Cloud Base Height

Shown below in Figures 3a and 3b are the calculated cloud base height for the 355 nm, 532 nm wavelengths. For the 355 nm, the number of positive and negative slopes was set to 10, while for the 532 nm the number of positive and negative slopes was set to 15. The number of positive and negative slopes will be used as a criterion to determine whether the peak detected is a cloud height or not. This value was varied to reduce the detection of noise as a cloud height. In Figure 3a the cloud at the height from 800 m to 1,200 m was detected. Unfortunately, the cloud located on the altitude range from 1,600m -1,800 m wasn't properly detected. One reason for this is that the peak at that point isn't high enough and the numbers of positive and negative slopes are too high. Reducing the criterion will lead to the increase in the detection of noises, which are now currently seen starting from 1,800 m above. For the 532 nm wavelength determination of the cloud heights of the 2 layers of clouds were achieved.

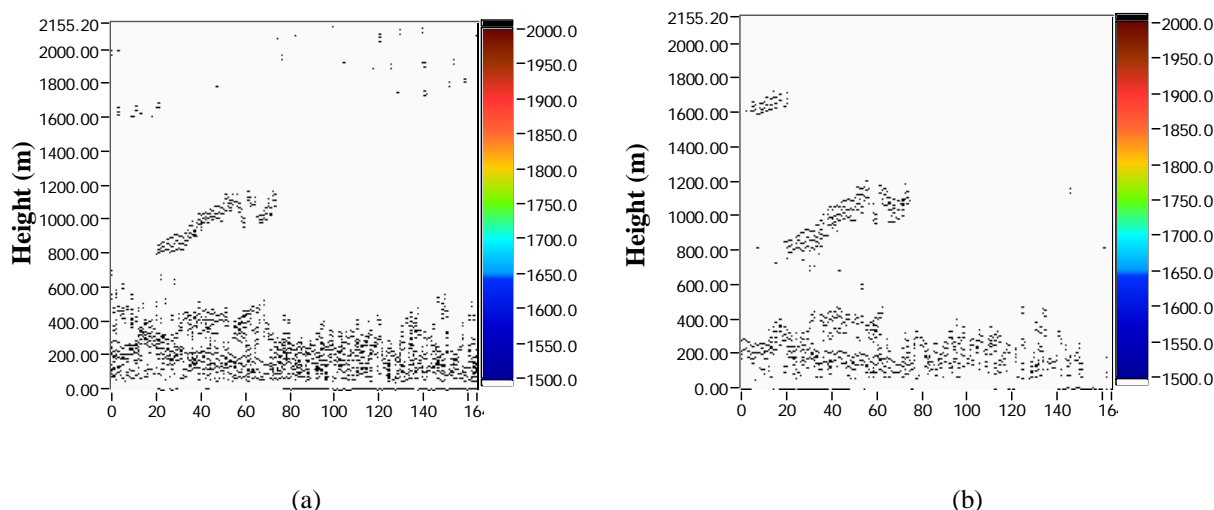


Figure 3. (a) Calculated cloud base height for 355 nm. (b) Calculated cloud base height for 532 nm.

4. CONCLUSION

LIDAR system provides a spatial and temporal variation of the boundary layer and cloud. The normalized concentration gradient method provides an estimate of the evolution of the BLH from our lidar data and from the slope of the RSCS, an automated method of determining the cloud based height can be achieved. Initial results indicate that during a period of stable stratification not much variation was observed in the BLH. Different methods in determining BLH must also be tried for our LIDAR system. Knowledge of the wind speed and wind direction is also needed to see the effect of sea breeze and land breeze especially with the location of our LIDAR system and the depolarization ratio obtained in the measurement. Continuous observation will be done as BLH is very important in air quality monitoring.

5. REFERENCES

- Boers, R., Eloranta, E.W., and Coulter, R.L., 1984: "LIDAR Observations of Mixed Layer Dynamics: Tests of Parameterized Entrainment Models of Mixed Layer Growth Rate", *Journal of Climate and Applied Meteorology*, Vol. 23, pp. 247–266.
- Coulter, R. L., 1979: "A Comparison of Three Methods for Measuring Mixing Layer Height", *Journal of Applied Meteorology*, Vol. 18, pp. 495-1499.
- Kunkel, K.E., Eloranta, E.W., and Shipley, S.T., 1977: "LIDAR Observations of the Convective Boundary Layer", *Journal of Applied Meteorology*, Vol. 16, pp. 1306–1311.
- Marsik, F.J., Fischer, K.W., McDonald, T.D., and Samson, P.J., 1995: "Comparison of the Methods for Estimating Mixing Height Used During the 1992 Atlanta Field Intensive", *Journal of Applied Meteorology*, Vol. 34, pp. 1802–1814.
- Melfi, S.H., Spinhirne, J.D., Chou, S.H., and Palm, S.P., 1985: "LIDAR Observations of the Vertically Organized Convection in the Planetary Boundary Layer Over the Ocean", *Journal of Climate and Applied Meteorology*, Vol. 24, pp. 806–821.

- Menut, L., Flamant, C., Pelon, J., Flamant, P.H., 1999: "Urban Boundary Layer Height Determination from LIDAR Measurements over the Paris Area", *Applied Optics*, Vol. 38, pp. 945–954.
- Sasano, Y., 1985: "Observational Study on the Atmospheric Mixed Layer and Transition Layer Structure Using a Mie LIDAR", *Journal of the Meteorological Society of Japan*, Vol. 63, pp. 419-435.
- Sasano, Y., Shigematsu, A., Shimizu H., Takeuchi, N. and Okuda, M., 1982: "On the Relationship between the Aerosol Layer Height and Mixed Layer Height Determined by Laser Radar and Low-level Radiosonde Observation", *Journal of Meteorological Society of Japan*, Vol. 60, pp. 889-895.
- Stull, R.B., 1988: *An Introduction to Boundary Layer Meteorology*, Kluwer Academic Publishers, Dordrecht, Netherlands, pp. 169-595.